DOI: 10.6060/ivkkt.20236606.6786

УДК: 537.525

О СРАВНЕНИИ МЕХАНИЗМОВ РЕАКТИВНО-ИОННОГО ТРАВЛЕНИЯ SiO_2 И Si_3N_4 В ПЛАЗМЕ HBr + Ar

А.М. Ефремов, В.Б. Бетелин, K.-H. Kwon

Александр Михайлович Ефремов (ORCID 0000-0002-9125-0763)*

Ивановский государственный химико-технологический университет, Шереметевский пр., 7, Иваново, Российская Федерация, 153000
E-mail: amefremov@mail.ru*

Владимир Борисович Бетелин (ORCID 0000-0001-6646-2660)

ФГУ ФНЦ НИИСИ РАН, Нахимовский пр., 36, к.1, Москва, Российская Федерация, 117218
E-mail: betelin@niisi.msk.ru

Kwang-Ho Kwon (ORCID 0000-0003-2580-8842)

Korea University, 208 Seochang-Dong, Chochiwon, Korea, 339-800
E-mail: kwonkh@korea.ac.kr

Исследовано влияние соотношения компонентов в смеси HBr + Ar на электрофизические параметры плазмы, стационарные концентрации активных частиц и кинетику реактивно-ионного травления (РИТ) SiO_2 и Si_3N_4 в условиях индукционного ВЧ (13,56 МГц) разряда. Совместное использование методов зондовой диагностики и моделирования плазмы показало, что увеличение доли аргона при постоянном давлении газа и вкладываемой мощности а) приводит к увеличению температуры электронов и концентраций заряженных частиц; б) сопровождается увеличением интенсивности ионной бомбардировки обрабатываемой поверхности; и в) вызывает близкое к пропорциональному снижение концентрации и плотности потока атомов брома. Найдено, что изменения скоростей травления SiO_2 и Si_3N_4 от состава смеси являются качественно подобными, при этом максимальные различия их абсолютных величин имеют место в плазме чистого HBr. Проведен анализ механизмов РИТ с использованием расчетных данных по плотностям потоков ионов и атомов брома. Установлено, что доминирующим механизмом травления SiO_2 является ионно-стимулированная химическая реакция, скорость которой в диапазоне 0–80% Ar остается практически постоянной за счет увеличения эффективной вероятности взаимодействия. Соответственно, заметная интенсификация физического распыления с ростом доли Ar в смеси вызывает лишь слабый рост наблюдаемой скорости РИТ. Напротив, основной вклад в процесс травления Si_3N_4 вносит физическое распыление, при этом скорость ионно-стимулированной химической реакции ограничивается низкой вероятностью взаимодействия. Это обеспечивает как меньшие абсолютные значения скоростей травления (особенно в области малых содержаний аргона), так и более резкую зависимость скорости РИТ от состава смеси.

Ключевые слова: HBr, плазма, параметры, активные частицы, ионизация, диссоциация, травление, кинетика, механизм

ON THE COMPARISON OF REACTIVE-ION ETCHING MECHANISMS FOR SiO_2 AND Si_3N_4 IN HBr + Ar PLASMA

A.M. Efremov, V.B. Betelin, K.-H. Kwon

Alexander M. Efremov (ORCID 0000-0002-9125-0763)*

Ivanovo State University of Chemistry and Technology, Sheremetevskiy ave., 7, Ivanovo, 153000, Russia
E-mail: amefremov@mail.ru

Vladimir B. Betelin (ORCID 0000-0001-6646-2660)
SRISA RAS, Nakhimovsky ave., 36, bld. 1, Moscow, 117218, Russia
E-mail: betelin@niisi.msk.ru

Kwang-Ho Kwon (ORCID 0000-0003-2580-8842)
Korea University, 208 Seochang-Dong, Chochiwon, Korea, 339-800
E-mail: kwonkh@korea.ac.kr

This work investigated the influence of component ratio in the HBr + Ar gas mixture on electro-physical plasma parameters, steady-state densities of active species and reactive-ion etching (RIE) kinetics for SiO_2 and Si_3N_4 under conditions of inductive RF (13.56 MHz) discharge. The combination of plasma diagnostics by Langmuir probes and plasma modeling indicated that an increase in Ar content at constant gas pressure and input power a) caused an increase in electron temperature and densities of charged species; b) results in increasing ion bombardment intensity; and c) leads to the nearly proportional decrease in Br atoms density and flux. It was found that variations of SiO_2 and Si_3N_4 etching rates vs. mixture composition are qualitatively similar while the maximum difference in corresponding absolute values takes place in pure HBr plasma. The analysis of RIE mechanisms was carried out using model-predicted data on fluxes of ions and bromine atoms. It was found that the dominant SiO_2 etching mechanism is the ion-assisted chemical reaction which is characterized by the nearly-constant rate in the range of 0–80% Ar due to an increase in the effective reaction probability. That is why the noticeable intensification of physical sputtering with increasing Ar fraction in a feed gas causes the only weak growth of obtained SiO_2 RIE rate. Oppositely, the Si_3N_4 etching process is mainly contributed by the physical sputtering while the efficiency of ion-stimulated chemical reaction is limited by the low reaction probability. This provides both slower etching process (especially in Ar-poor plasmas) and stronger sensitivity of etching rate to the change in mixture composition.

Key words: HBr, plasma, parameters, active species, ionization, dissociation, etching, kinetics, mechanism

Для цитирования:
Ефремов А.М., Бетелин В.Б., Kwon K.-H. О сравнении механизмов реактивно-ионного травления SiO_2 и Si_3N_4 в плазме HBr + Ar. *Изв. вузов. Химия и хим. технология*. 2023. Т. 66. Вып. 6. С. 37–45. DOI: 10.6060/ivkkt.20236606.6786.

For citation:
Efremov A.M., Betelin V.B., Kwon K.-H. On the comparison of reactive-ion etching mechanisms for SiO_2 and Si_3N_4 in HBr + Ar plasma. *ChemChemTech* [*Izv. Vyssh. Uchebn. Zaved. Khim. Khim. Tekhnol*.]. 2023. V. 66. N 6. P. 37–45. DOI: 10.6060/ivkkt.20236606.6786.

INTRODUCTION

In our days, the silicon-based electronics still occupies the dominant position in the world-wide production of micro- and nano-electronic devices. Among many materials involved in the technology of silicon-based integrated electronic circuits, a significant role belongs to silicon dioxide (SiO_2) and/or silicon nitride (Si_3N_4). In particular, these two "workhorses" are used as gate dielectrics in field-effect transistors, inter-element insulating spacers, planar insulating and passivating layers in multi-layer structures as well hard mask materials in some lithography applications [1]. Obviously, the most of above applications require the precision patterning (dimensional etching) of preliminary deposited SiO_2 and Si_3N_4 layers with both keeping their original dielectric properties and satisfying the strong requirements to etching profile features. Therefore, the development and optimization of corresponding etching techniques is an important task to provide advanced device technologies and functional characteristics.

From many published works (see, for example, Refs. [2-4]), it can be understood that the widely used tool for the patterning of silicon and silicon-containing compounds is the reactive-ion etching (RIE) with using low-pressure fluorocarbon gas plasmas. Up to now, all principal features of fluorine-based etching chemistry in respect to Si, SiO_2 and Si_3N_4 have been studied with enough details, and corresponding etching mechanisms are well-understood. In particular, it was shown that the heterogeneous reaction $Si + xF \rightarrow SiF_x$ exhibits the spontaneous mechanism that produces both high etching rate and nearly isotropic etching profile [4, 5]. Oppositely, the interaction of fluorine atoms with SiO_2 and Si_3N_4 has the nature of ion-assisted process where

the ion bombardment initiates chemical reaction through the destruction of Si-O or Si-N bonds [5, 6]. On this background, the much less research attention was paid to alternate etching chemistries, and namely to the bromine-based chemistry provided by the HBr gas. At the same time, Refs. [7, 8] reported that the use of HBr-containing plasmas allows one to achieve the highly-anisotropic etching of both mono- and poly-Si due to the negligible spontaneous reaction between Si and Br atoms. The last effect is normally attributed to the bigger size of Br atom that retards its penetration into the Si lattice. As a result, the reaction $Si + xBr \rightarrow SiBr_x$ involves the limited amount of Si atom bonds and thus, leads to the formation of non-saturated and low-volatile reaction products which can be desorbed only by the ion bombardment. Another important feature is that the HBr-rich plasma provides the higher etching selectivity of silicon in respect to organic photoresist masks. The reason is that the ultra-violet (~110-210 nm) irradiation from excited HBr molecules causes the hardening of the photoresist surface due to additional cross-linking and graphitization [9].

Unfortunately, the existing data on etching kinetics for both SiO_2 and Si_3N_4 in HBr-containing plasmas are not enough to make an adequate conclusion concerning advantages and/or drawbacks of such gas systems in comparison with fluorocarbon plasmas. In order to improve the situation, we have compared RIE processes for SiO_2 in CF_4 + Ar and и HBr +Ar plasmas under identical processing conditions [10]. The most important findings were that a) the SiO_2 etching rate in both gas systems is not limited by ion-driven process (at least at ion bombardment energies of ~ 400 eV); b) the variations of Ar fraction in a feed gas produces similar responses in densities of main active species and SiO_2 etching rates; and c) the HBr + Ar plasma is features by higher Br atom flux, but by slower SiO_2 etching process. The aim of present work was the compare etching behaviors of SiO_2 and Si_3N_4 in the HBr + Ar plasma with different HBr/Ar mixing ratios. The latter was chosen as a single variable parameter because it directly reflects the transition between physical and chemical etching pathways, and thus allows one the better understanding features of corresponding etching mechanisms. Accordingly, main goals were a) to investigate the possibility of HBr/Ar mixing ratio to control SiO_2 and Si_3N_4 etching rates and selectivities; b) to find relationships between feed gas composition, gas-phases plasma characteristics and RIE kinetics; and c) to formulate both common features and differences in corresponding etching mechanisms.

EXPERIMENTAL AND MODELING DETAILS

Experimental setup and procedures

Both plasma diagnostics and etching experiments were performed in the planar inductively coupled plasma (ICP) reactor known from our previous works [6, 10, 11]. Plasma in the HBr + Ar gas mixture was excited using the 13.56 MHz power supply while another 13.56 MHz rf generator was powered the bottom electrode (the substrate holder) to produce the negative bias potential, $-U_{dc}$. The latter was measured using the high-voltage probe (AMN-CTR, Youngsin Eng.). Constant processing conditions were total gas flow rate (q = 40 sccm), gas pressure (p = 4 mtor), input power (W = 700 W, or 0.7 W/cm^3) and bias power (W_{bias} = 300 W). Accordingly, the variable input parameter was the Ar fraction in a feed gas (y_{Ar} = 0-80%) adjusted through partial flow rates for component gases.

Electro-physical plasma parameters were measured using the double Langmuir probe tool (DLP2000, Plasmart Inc.). The probe was installed through the special viewport on chamber wall as well as was centered in the radial position. The distance between the probe tip and the bottom electrode was ~ 5 cm. The treatment of raw voltage-current (I-V) accounted for well-known statements of Langmuir probe theory in low pressure plasmas [5, 12]. As a result, we obtained data on electron temperature (T_e) and ion current density (J_+). In preliminary experiments, it was found also that the presence of treated material in the reactor chamber (as well as an increase in the sample size up to 5 times compared with convenient ones) does not disturb the shape of I-V curves and thus, does not influence plasma parameters determining electron impact kinetics. In fact, this allows one to neglect the effect of reaction products on the steady-state plasma condition and thus, to consider the gas phase as the unperturbed source of active species. Another important feature is that both I-V curves and related plasma parameters were not sensitive to changes in bias power. Therefore, our experimental setup and processing conditions correspond to the "classical" ICP system with the independent adjustment of species densities (by the input power source, W) and ion bombardment energy (by the bias power source, W_{bias}). In addition, since the ion density at the plasma sheath edge for both plasma/probe and plasma/bottom electrode interfaces is controlled by identical chemical and transport processes, one can roughly equalize ion fluxes passed through corresponding sheath regions [5]. Accordingly, the ion flux coming from a gas phase to the etched surface may simply be evaluated as $\Gamma_+ \approx J_+/e$ [6, 13-15].

Etching kinetics of SiO_2 and Si_3N_4 were studied using fragments of Si (111) wafer with an average size of ~ 2×2 cm with preliminary deposited oxide and nitride layers. Deposition details may be found in Ref. [6]. The small sample size allowed one to exclude the loading effect and thus, to obtain etching rates which adequately reflects heterogeneous process kinetics. Etched samples were placed in the middle part of the bottom electrode while the temperature of electrode was stabilized at ~ 17 °C using the built-in water-flow cooling system. In order to determine etching rates, a part of each sample was covered by the photoresist mask (AZ1512, positive) with a thickness of ~ 1.5 μm. The last value was more than enough to provide the stable mask layer within typical processing times. It should be mentioned also that the mask etching rate was very small, almost negligible. This fact evidently reflects the feature of HBr-containing plasmas discussed in Ref. [9]. After finishing the etching process, the mask was removed in organic solvents. Finally, we measured the step Δh between masked and non-masked sample areas using the surface profiler Alpha-Step 500 (Tencor) and then, calculated the etching rate as $R = \Delta h/\tau$, where $\tau = 5$ min is the processing time. Preliminary experiments indicated that the condition $\tau < 5$ min surely provides nearly linear kinetic curves $\Delta h = f(\tau)$ and thus, corresponds to the steady-state etching regime for both materials. In addition, nearly linear kinetic serve also as an indirect proof of the constant sample temperature. Otherwise, one could expect the faster-than-linear (the Arrhenius-like) growth of Δh toward higher processing times due to an increase in sample temperature.

Plasma modeling

In order to obtain densities and fluxes of plasma active species, we applied 0-dimensional (global) plasma model. The model content, approaches and kinetic scheme (the set of chemical reactions with corresponding rate coefficients) were the same as have been used in our previous works dealt with HBr + Ar plasmas under typical RIE conditions [13, 14]. Basic assumptions were as follows:

1) The electron energy distribution function (EEDF) has the nearly Maxwellian shape. Such an approach is widely used for the modeling of low-pressure ($p < 20$ mtor) high-density ($n_+ > 10^{10}$ cm^{-3}, where n_+ is the total positive ion density) plasmas in different molecular gases [5]. The reason is that the high ionization degree for gas species ($n_+/N > 10^{-4}$, where $N = p/k_BT_{gas}$ is the gas density at the gas temperature of T_{gas}) provides the sufficient contribution of equilibrium electron-electron collisions to the overall electron energy loss. Though this fact has no direct confirmation for HBr + Ar gas system, we can simply refer for the quite good agreement between measured and model-predicted ion current densities obtained in Ref. [13] with Maxwellian EEDF. Since the measured J_+ is contributed by partial currents (and thus, by partial densities) of several molecular and atomic ions, one can surely assume the correct description of electron-impact kinetics for basic processes, such as dissociation and ionization. That is why we determined corresponding rate coefficients using fitting expressions $k = f(T_e)$ [14] obtained after the integration of Maxwellian EEDF with corresponding process cross-section.

2) The total density of positive ions is connected with the measured ion current density as $J_+ \approx \approx 0.61en_+\upsilon_B$ [5], where $\upsilon_B = (eT_e/m_i)^{1/2}$ is the ion Bohm velocity, and m_i is the effective ion mass. The latter may be estimated assuming that the fraction of each ion inside n_+ is proportional to the ionization rate for corresponding neutral component.

3) The electron density is connected with n_+ through the kinetic equation for negative ions and quasi-neutrality condition. This allows one to obtain $n_e \approx k_3n_+^2/(k_3n_+ + k_1[HBr] + k_2[Br_2])$, where rate coefficients k_1, k_2 and k_3 are for R1: $HBr + e \rightarrow H + Br^-$; R2: $Br_2 + e \rightarrow Br + Br^-$ and R3: $Br^- + X^+ \rightarrow$ neutral products.

4) The heterogeneous recombination of Br and H atoms appears as the first-order chemical reaction in respect to their gas-phase densities. Corresponding rate coefficients are $k \approx (r+l)\gamma\upsilon_T/2rl$ [15], where r and l are inner sizes of the cylindrical reactor chamber, υ_T is the thermal velocity, and γ is the recombination probability [13, 14].

5) The gas temperature was assumed be equal to 600 K and independent on the HBr/Ar mixing ratio [10, 13, 14]. The absolute value was derived from Ref. [16], where T_{gas} was measured in pure HBr plasma as a function of gas pressure and input power. In fact, it looks quite typical for the reactor of given geometry and input power density. The condition $T_{gas} \approx$ const follows from the nearly constant temperature of external chamber wall. As the latter adequately traces changes in the input power, the above suggestion seems to be correct.

RESULTS AND DISCUSSION

From plasma diagnostics using by Langmuir probes, it was found that that an increase in Ar mixing ratio results in increasing both electron temperature (T_e = 3.1-3.5 eV for 0-80% Ar) and ion current density (J_+ = 1.7-5.0 mA/cm^2 for 0-80% Ar) (Fig. 1(a)).

The mentioned change in T_e is surely connected with a decrease in the overall electron energy

loss during the substitution of molecular gas for the atomic one. Obviously, since the first excitation potential for Ar atoms exceeds 11 eV [17, 18], an increase in y_{Ar} cannot compensate for decreasing energy losses in low-threshold vibrational and electronic excitations of HBr molecules. The growth of J_+ traces same changes in both ion Bohm velocity and total density of positive ions ($n_+ = 9.2\cdot10^{10}$-$1.9\cdot10^{11}$ cm^{-3} for 0-80% Ar, see Fig. 1(b)). The latter reflects the behavior of the total ionization rate that is provided by increasing ionization rate coefficients for neutral species and electron density ($n_e = 5.1\cdot10^{10}$-$1.7\cdot10^{11}$ cm^{-3} for 0-80% Ar, see Fig. 1(b)). Accordingly, the growth of electron density is provided by decreasing rates of R1 and R2 (that is also reflected on decreasing plasma electronegativity) under the condition of the nearly constant total ionization frequency. From Fig. 1(c), it can be seen also that an increase in y_{Ar} lowers the negative bias potential ($-U_{dc}$ = 385-286 V for 0-80% Ar), in spite of W_{dc} = const. Such situation is because increasing ion flux $\Gamma_+ \approx J_+/e$ partially compensates for the negative charge produced by the bias power source. At the same time, the decreasing tendency for the ion bombardment energy appears to be weaker compared with the growth of ion flux. As results, one can obtain an increase in the ion bombardment intensity toward Ar-rich plasmas, as it follows from the change of $(M_i\varepsilon_i)^{1/2}\Gamma_+$ [10, 11, 19] (Fig. 1(c)).

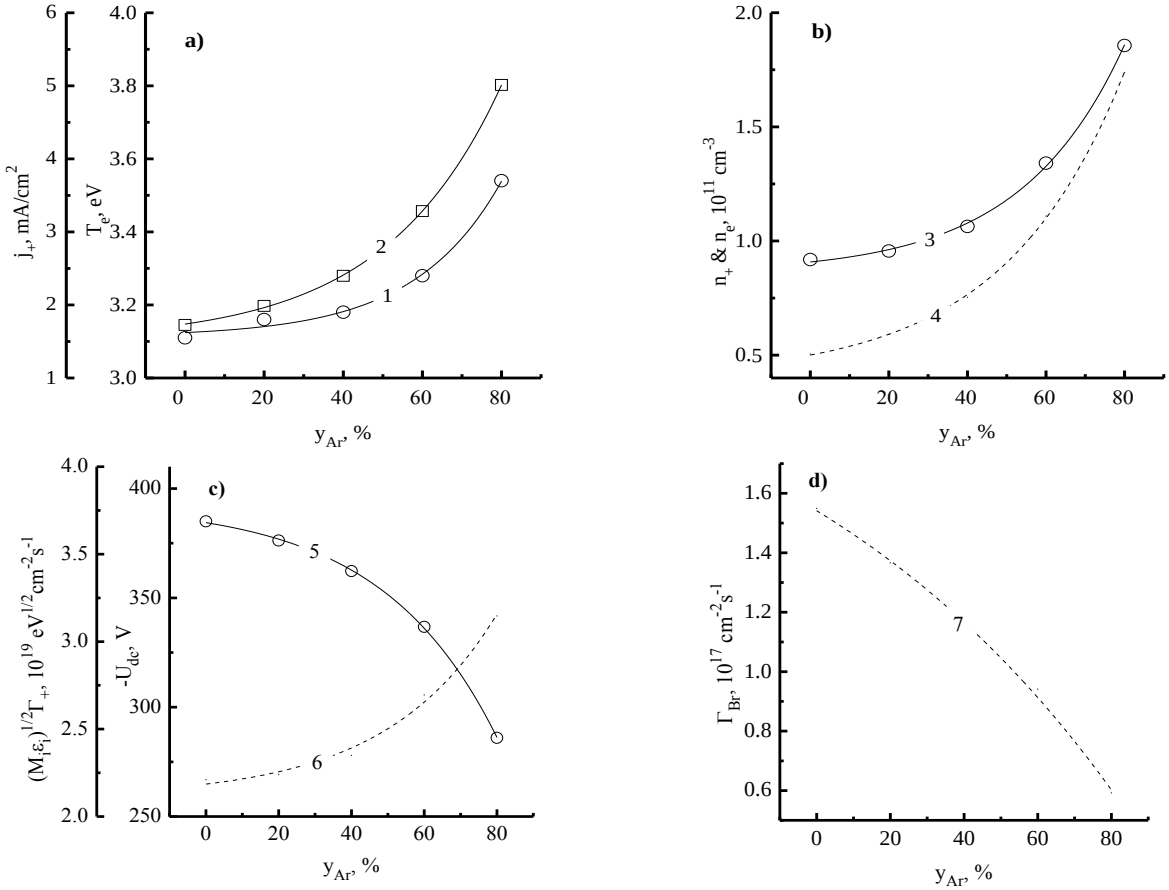

Fig. 1. Measured (solid lines + symbols) and model-predicted (dashed lines) plasma parameters as functions of Ar fraction in HBr + Ar mixtures at p = 4 mtor, W = 700 W and W_{dc} = 300 W: 1 – electron temperature; 2 – ion current density; 3 – total positive ion density; 4 – electron density; 5 – negative dc bias on the lower electrode; 6 – parameter $(M_i\varepsilon_i)^{1/2}\Gamma_+$ characterizing the ion bombardment intensity; and 7 – Br atom flux

Рис. 1. Измеренные (сплошная линия + точки) и расчетные (пунктирная линия) параметры плазмы в зависимости от доли Ar в смеси HBr + Ar при p = 4 мтор, W = 700 Вт и W_{dc} = 300 Вт: 1 – температура электронов; 2 – плотность ионного тока; 3 – суммарная концентрация положительных ионов; 4 – концентрация электронов; 5 – отрицательное смещение на нижнем электроде; 6 – параметр $(M_i\varepsilon_i)^{1/2}\Gamma_+$ характеризующий интенсивность ионной бомбардировки; и 7 – плотность потока атомов Br

The model-based analysis of neutral species kinetics confirms basic features of HBr plasma known from previous studies [13, 14, 20, 21]. These are as follows:

1) The formation of Br atoms is provided by R4: HBr + e → H + Br + e and R5: Br_2 + e → 2Br + e with nearly equal rates. The principal role of R5 is due to both $k_4 < k_5$ (~ $2.8\cdot10^{-9}$ cm^3/s for k_4 vs. ~ $1.6\cdot10^{-8}$ cm^3/s

for k_5 at T_e = 4 eV) and quite high density of Br_2 molecules. The latter is maintained by the effective recombination of Br atoms on chamber walls as R7: Br + Br → → Br_2 [13, 14]. Accordingly, heterogeneous processes R7 and R8: Br + H → HBr represent the dominant loss mechanism for bromine atoms.

2) The total H atom loss rate in gas-phase reactions R9: H + HBr → H_2 + Br ($k_9 \sim 6.5 \cdot 10^{-12}$ cm^3/s) and R10: H + Br_2 → HBr + Br ($k_{10} \sim 6.0 \cdot 10^{-11}$ cm^3/s) exceeds the rate of their heterogeneous recombination in R11: H + H → H_2 and R12: H + Br → HBr. Taking into account that both R6 and R7 represent additional sources of Br atoms, the condition [H] << [Br] surely takes place.

3) The effective reproduction of HBr molecules in R8 and R10 causes the quite low dissociation degree of these species. That is why HBr remains to be the dominant gas-phase component.

As the HBr/Ar mixing ratio changes toward Ar-rich plasmas, the Br atom density decreases slower (by ~ 2.5 times for 0-80% Ar) than it can be expected from the change of (1-y_{Ar}). Such situation results from increasing efficiency of R4 and R5 (($k_4 + k_5$)n_e = 99-431 s^{-1} for 0-80% Ar) due to the simultaneous change in electron temperature and electron density. Accordingly, the same behavior is also for the Br atom flux, as shown in Fig. 1(d). Therefore, the brief summary from data of Fig. 1 is that an increase in y_{Ar} intensifies the ion bombardment, suppresses the chemical etching pathway through decreasing flux of etchant species as well as results in increasing neutral/charged ratio (Γ_{Br}/Γ_+ = 14.4-4.6 for 0-80% Ar). The latter means that increasing contribution of directional etching component creates the favorable condition for achieving the more anisotropic etching profile.

From etching experiments, it was found that both SiO_2 and Si_3N_4 etching rates demonstrate the monotonic growth with increasing Ar fraction in a feed gas, and their absolute values became to be closer in Ar-rich plasma (Figs. 2(a,b)). Therefore, the difference between corresponding sputtering yields seems to be lower than that for effective reaction probabilities. In earlier works, it was shown that the experimentally obtained RIE rate, R, represents the combination of two summands, such as the rate of physical sputtering R_{phys} (since under typical RIE conditions the ion bombardment energy exceeds the sputtering threshold for etched material) and the rate of ion-assisted chemical reaction R_{chem} [10, 11, 22]. In order to evaluate contributions of these etching pathways, we measured SiO_2 and Si_3N_4 etching rates in pure Ar plasma $R_{phys,Ar}$, calculate corresponding sputtering yields as $Y_{S,Ar}$ = $R_{phys,Ar}/\Gamma_+$ (~ 0.03 for both SiO_2 and Si_3N_4 at ion energy of 230 eV) and then, determined actual sputtering yields for HBr + Ar plasma as $Y_S = Y_{S,Ar}(m_i/m_{Ar})^{1/2}$. Accordingly, these allow one to obtain $R_{phys} = Y_S\Gamma_+$ and $R_{chem} = R - R_{phys}$ [10].

Data of Fig. 2(a) clearly indicate that, in the case of SiO_2, the condition $R_{chem} > R_{phys}$ surely takes place. In fact, this means that the dominant etching mechanism is the ion-assisted chemical reaction, but the reaction rate keeps the nearly constant value in the range of 0-80% Ar. The latter is because a decrease in Br atom flux is compensated by the growth of effective reaction probability $\gamma_R = R_{chem}/\Gamma_{Br}$ (Fig. 2(c)). As a result, the acceleration of physical sputtering with increasing Ar fraction in a feed gas (6.1-17.8 nm/min, or by ~ 3 times for 0-80% Ar) has the only weak influence on the overall SiO_2 etching rate (40.0-54.6 nm/min for 0-80% Ar). From the comparison of Figs. 1(c) and 2(c), it can be seen also that the change of γ_R toward Ar-rich plasmas correlates with increasing ion bombardment intensity. In our opinion, such situation reflects the activation of chemical reaction through oxide bond breaking. In addition, since behaviors of both R_{chem} and R contradict to Γ_{Br}, but follows the change of $(M_i\varepsilon_i)^{1/2}\Gamma_+$, the ion-flux-limited etching regime does work. In the case of Si_3N_4, one can obtain $R_{chem} < R_{phys}$ (Fig. 2(b)) as well as the almost identical changes of R and R_{phys} with increasing Ar fraction in a feed gas. Therefore, the dominant etching mechanism is the physical sputtering while the efficiency of chemical etching pathway is limited by the low (by more than 10 times less compared with γ_R for SiO_2, see Fig. 2(d)) reaction probability. In our opinion, the last effect may be connected with a) the lower sticking probability of Br atoms to Si_3N_4 surface; and/or b) the denser structure of Si_3N_4 material that causes the worse penetration of etchant species inside the bulk material. As a result, Si_3N_4 demonstrates lower, compared to SiO_2, absolute etching rates (especially in HBr-rich plasmas) as well as the stronger sensitivity to the change in mixture composition through the ion bombardment intensity. Finally, we would like to note that the parameter γ_R describes only formal relationships between etching rate and the flux of etchant species. Actually, the dependence of γ_R on processing conditions represents the overall effect from various plasma-related factors which accelerate or retard the etching process. Except the ion bombardment, these may be, for example, the ultra-violet radiation from excited particles, the adsorption of non-reactive species that passivates the surface, chemical reactions with components of etched material (in our case, with O and N atoms) as well as many other

ones which can only be suggested, but not known exactly. That is why the above discussion around Figs. 2(c, d) provides the simplest (though quite reasonable) explanation for experimentally obtained effects.

The alternate approach to the analysis of plasma etching kinetics assumes RIE process as the chemically-assisted physical sputtering [23, 24]. In particular, it is believed that the interaction of etchant species with surface atom reduces the number of chemical bonds with its neighborhood and thus, lowers the sputtering threshold. The kinetic characteristic of such process is the etching yield, $Y_R = R/\Gamma_+$ [23]. From Fig. 2(c), it can be understood that the parameter Y_R for SiO_2 is much higher than the experimentally obtained sputter yield in the Ar plasma. As such, one can suggest that ions really sputter not the original SiO_2 surface, but partially brominated Si atoms (in fact, non-saturated $SiBr_x$ compounds). A decrease in Y_R toward Ar-rich plasmas is associated with the change in the ion bombardment energy, as it follows from the behavior of $-U_{dc}$ (Fig. 1(c)). In the case of Si_3N_4, the lower reaction probability limits the surface bromination rate and, probably, reduces the fraction of etched surface covered by reaction products. That is why ions impact mostly the original Si_3N_4 material while the parameter Y_R reaches typical sputter yield values (Fig. 2(d)). A constancy of Y_R in the range of 0-80% Ar is because a decrease in the ion bombardment energy is compensated by an increase in γ_R. This causes an increase in the surface bromination rate (see the behavior of R_{chem} in Fig. 2(b)) even under the condition of decreasing Br atom flux.

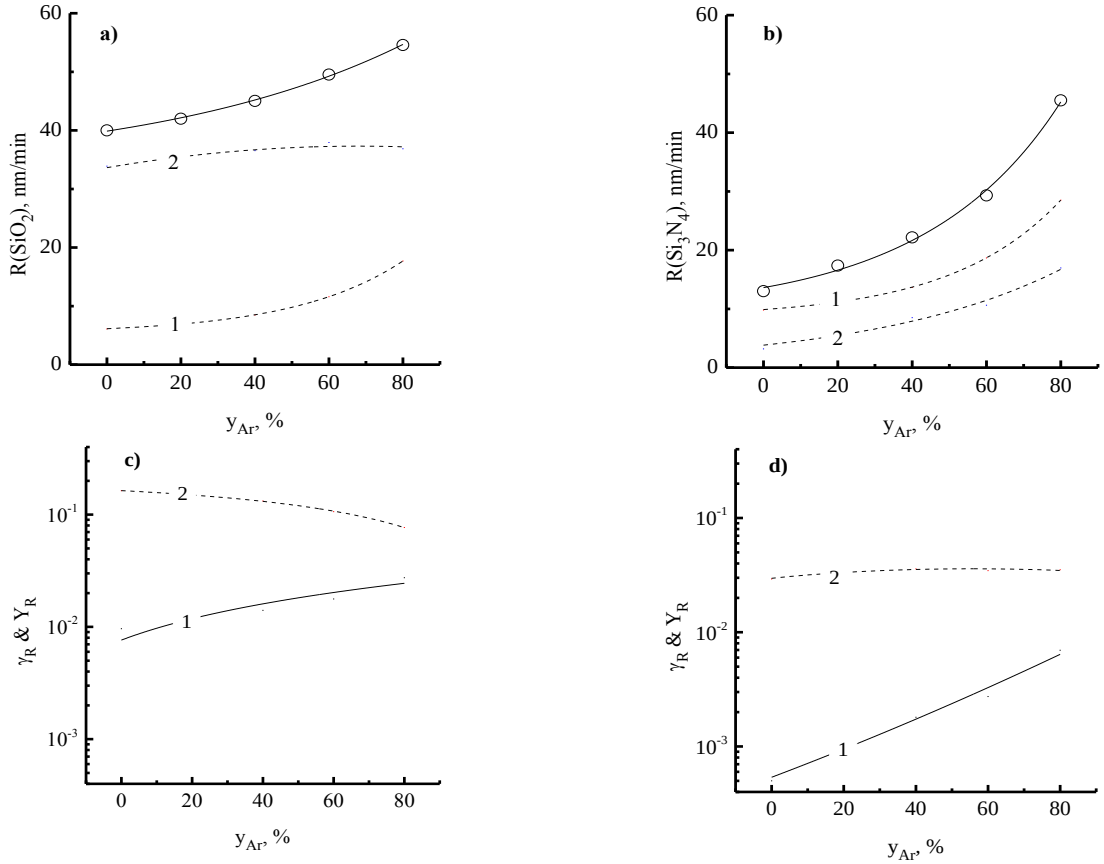

Fig. 2. Etching rates (a, b) and kinetic characteristics of heterogeneous processes (c, d) for SiO_2 (a, c) and Si_3N_4 (b, d) in HBr + Ar mixtures at p = 4 mtor, W = 700 W and W_{dc} = 300 W. In Figs. a) and b): 1 – rate of physical sputtering (R_{phys}); and 2 – rate of ion-assisted chemical reaction (R_{chem}). In Figs. c) and d): 1 – effective reaction probability (γ_R); 2 – etching yield (Y_R)

Рис. 2. Скорости травления (a, b) и кинетические характеристики гетерогенных процессов (c, d) для SiO_2 (a, c) и Si_3N_4 (b, d) в смеси HBr + Ar при p = 4 мтор, W = 700 Вт и W_{dc} = 300 Вт. На рис. a) и b): 1 – скорость физического распыления (R_{phys}); и 2 – скорость ионно-стимулированной химической реакции (R_{chem}). На рис. c) и d): 1 – эффективная вероятность взаимодействия (γ_R); 2 – выход травления (Y_R)

CONCLUSIONS

In this work, we compared reactive-ion etching kinetics as well as attempted to determine features of etching mechanisms for SiO_2 and Si_3N_4 in the HBr + Ar plasma. The use of HBr/Ar mixing ratio as the variable parameter was because it directly reflects the transition between chemical and physical etching pathways. The

combination of plasma diagnostics by Langmuir probes with the 0-dimensional plasma model provided data on steady-state plasma parameters and densities of active species. It was found that the transition toward Ar-rich plasmas increases both electron temperature and plasma density, intensifies the ion bombardment as well as suppresses the Br atom density proportionally to the change in y_{Ar}. The analysis of etching kinetics indicated that the dominant SiO_2 etching mechanism is the ion-assisted chemical reaction with the nearly-constant rate in the range of 0-80% Ar. The latter is because a decrease in Br atom flux is compensated by increasing reaction probability. As a result, the acceleration of physical sputtering with increasing Ar fraction in a feed gas causes the only weak growth of the overall SiO_2 etching rate. Oppositely, the Si_3N_4 etching process is mainly contributed by the physical sputtering while the efficiency of chemical etching pathway is limited by the low reaction probability. As a result, one can obtain lower, compared to SiO_2, absolute etching rates as well as the stronger sensitivity to the change in mixture composition through the ion bombardment intensity.

The publication was made within the framework of the state task of the Federal State Institution Scientific Research Institute for System Analysis, Russian Academy of Sciences (conducting fundamental scientific research (47 GP)) on the topic No. 11021060909091-4-1.2.1 "Fundamental and applied research in the field of lithographic limits of semiconductor technologies and physicochemical processes of etching 3D nanometer dielectric structures for the development of critical technologies for the production of electronic components. Research and construction of models and designs of microelectronic elements in an extended temperature range (from -60 °C to +300 °C) (FNEF-2022-0006)".

The authors declare the absence a conflict of interest warranting disclosure in this article.

Публикация выполнена в рамках государственного задания ФГУ ФНЦ НИИСИ РАН (Проведение фундаментальных научных исследований (47 ГП)) по теме НИР «11021060909091-4-1.2.1 Фундаментальные и прикладные исследования в области литографических пределов полупроводниковых технологий и физико-химических процессов травления 3D нанометровых диэлектрических структур для развития критических технологий производства ЭКБ. Исследование и построение моделей и конструкций элементов микроэлектроники в расширенном диапазоне температур (от -60 °C до +300 °C) (FNEF-2022-0006)».

Авторы заявляют об отсутствии конфликта интересов, требующего раскрытия в данной статье.

REFERENCES
ЛИТЕРАТУРА

1. **Iwai H., Ohmi S.** Silicon integrated circuit technology from past to future. *Microelectron. Reliabil.* 2002. V. 42. N 4–5. P. 465-491. DOI: 10.1016/S0026-2714(02)00032-X.
2. **Nojiri K.** Dry etching technology for semiconductors. Tokyo: Springer Internat. Publ. 2015. 116 p. DOI: 10.1007/978-3-319-10295-5.
3. Advanced plasma processing technology. New York: John Wiley & Sons Inc. 2008. 479 p.
4. **Wolf S., Tauber R.N.** Silicon Processing for the VLSI Era. V. 1. Process Technology. New York: Lattice Press. 2000. 416 p.
5. **Lieberman M.A., Lichtenberg A.J.** Principles of plasma discharges and materials processing. New York: John Wiley & Sons Inc. 2005. 757 p. DOI: 10.1002/0471724254.
6. **Efremov A., Lee B. J., Kwon K.-H.** On relationships between gas-phase chemistry and reactive-ion etching kinetics for silicon-based thin films (SiC, SiO_2 and Si_xN_y) in multicomponent fluorocarbon gas mixtures. *Materials.* 2021. V. 14. P. 1432(1-27). DOI: 10.3390/ma14061432.
7. **Bestwick T.D., Oehrlane G.S.** Reactive ion etching of silicon using bromine containing plasmas. *J. Vac. Sci. Technol. A.* 1990. V. 8. P. 1696-1701. DOI: 10.1116/1.576832.
8. **Jin W., Vitale S.A., Sawin H.H.** Plasma-surface kinetics and simulation of feature profile evolution in Cl_2+HBr etching of polysilicon. *J. Vac. Sci. Technol.* 2002. V. 20. P. 2106-2114. DOI: 10.1116/1.1517993.
9. **Pargon E., Menguelti K., Martin M., Bazin A., Chaix-Pluchery O., Sourd C., Derrough S., Lill T., Joubert O.** Mechanisms involved in HBr and Ar cure plasma treatments applied to 193 nm photoresists. *J. Appl. Phys.* 2009. V. 105. P. 094902. DOI: 10.1063/1.3116504.
10. **Efremov A.M., Murin D.B., Betelin V.B., Kwon K.-H.** Special Aspects of the Kinetics of Reactive Ion Etching of SiO_2 in Fluorine-, Chlorine-, and Bromine-Containing Plasma. *Russ. Microelectron.* 2020. V. 49. N 2. P. 94-102. DOI: 10.1134/S1063739720010060.
11. **Efremov A.M., Rybkin V.V., Betelin V.B., Kwon K.-H.** On mechanisms of oxygen influence on gas-phase parameters and silicon reactive-ion etching kinetics in HBr+ Cl_2+ O_2 plasma. *ChemChemTech [Izv. Vyssh. Uchebn. Zaved. Khim. Khim. Tekhnol.]*. 2019. V. 62. N 10. P. 76-83. DOI: 10.6060/ivkkt.20196210.6046.
Ефремов А.М., Рыбкин В.В., Бетелин В.Б., KwonK.-H. О механизмах влияния кислорода на параметры газовой фазы и кинетику реактивно-ионного травления кремния в плазме HBr+ Cl_2+ O_2. *Изв. вузов. Химия и хим. технология.* 2019. Т. 62. Вып. 10. С. 76-83. DOI: 10.6060/ivkkt.20196210.6046.
12. **Shun'ko E.V.** Langmuir probe in theory and practice. Boca Raton: Universal Publ. 2008. 245 p.
13. **Kwon K.-H., Efremov A., Kim M., Min N. K., Jeong J., Kim K.** A model-based analysis of plasma parameters and composition in HBr/X (X=Ar, He, N_2) inductively coupled plasmas. *J. Electrochem. Soc.* 2010. V. 157. N 5. P. H574-H579. DOI: 10.1149/1.3362943.

14. **Efremov A., Lee J., Kwon K.H.** A comparative study of CF_4, Cl_2 and HBr + Ar inductively coupled plasmas for dry etching applications. *Thin Solid Films.* 2017. V. 629. P. 39-48. DOI: 10.1016/j.tsf.2017.03.035.
15. **Miakonkikh A., Kuzmenko V., Efremov A., Rudenko K.** A comparison of CF_4, $CBrF_3$ and $C_2Br_2F_4$ Plasmas: Physical parameters and densities of atomic species. *Vacuum*. 2022. V. 200. P. 110991 (1-7). DOI: 10.1016/j.vacuum.2022.110991.
16. **Cunge G., Ramos R., Vempaire D., Touzeau M., Neijbauer M., Sadeghi N.** Gas temperature measurement in CF_4, SF_6, O_2, Cl_2, and HBr inductively coupled plasmas. *J. Vac. Sci. Technol. A.* 2009. V. 27. P. 471-478. DOI: 10.1116/1.3106626.
17. **Raju G.G.** Gaseous electronics. Tables, Atoms and Molecules. Boca Raton: CRC Press. 2012. 790 p. DOI: 10.1201/b11492.
18. **Christophorou L.G., Olthoff J.K.** Fundamental electron interactions with plasma processing gases. New York: Springer Science+Business Media LLC. 2004. 776 p. DOI: 10.1007/978-1-4419-8971-0.
19. **Efremov A., Murin D., Kwon K.-H.** Concerning the Effect of Type of Fluorocarbon Gas on the Output Characteristics of the Reactive-Ion Etching Process. *Russ. Microelectron.* 2020. V. 49. N 3. P. 157-165. DOI: 10.1134/S1063739720020031.
20. **Lee J., Efremov A., Lee B.J., Kwon K.-H.** Etching Characteristics and Mechanisms of TiO_2 Thin Films in CF_4 + Ar, Cl_2 + Ar and HBr + Ar Inductively Coupled Plasmas. *Plasma Chem. Plasma Process.* 2016. V. 36. N 6. P. 1571-1588. DOI: 10.1007/s11090-016-9737-y.
21. **Efremov A., Kim Y., Lee H.W., Kwon K.-H.** A Comparative Study of HBr-Ar and HBr-Cl_2 Plasma Chemistries for Dry Etch Applications. *Plasma Chem. Plasma Process.* 2011. V. 31. N 2. P. 259-271. DOI: 10.1007/s11090-010-9279-7.
22. **Gray D.C., Tepermeister I., Sawin H.H.** Phenomenological modeling of ion enhanced surface kinetics in fluorine-based plasma etching. *J. Vac. Sci. Technol. B.* 1993. V. 11. P. 1243-1257. DOI: 10.1116/1.586925.
23. **Vitale S.A., Chae H., Sawin H.H.** Silicon etching yields in F_2, Cl_2, Br_2, and HBr high density plasmas. *J. Vac. Sci. Technol. A.* 2001. V. 19. P. 2197-2206. DOI: 10.1116/1.1378077.
24. **Tachi S., Okudaira S.** Chemical sputtering of silicon by F^+, Cl^+, and Br^+ ions: Reactive spot model for reactive ion etching. *J. Vac. Sci. Technol. B.* 1986. V. 4. P. 459-487. DOI: 10.1116/1.583404.

Поступила в редакцию 16.12.2022
Принята к опубликованию 14.03.2023

Received 16.12.2022
Accepted 14.03.2023